Arch Biol Sci. 2024;76(3):325-333 https://doi.org/10.2298/ABS240707024Q

A novel lidocaine-chitosan-barium titanate microemulsion gel for prolonged local anesthesia: An *in vitro* study

Xiaoru Qiao and Ling Li*

Department of Anesthesiology, Ankang Central Hospital, Ankang City, Shaanxi Province, 725000, China

***Corresponding author**: 13488208879cc@sina.com

Received: July 7, 2024; **Revised**: July 23, 2024; **Accepted**: July 24, 2024; **Published online**: August 16, 2024

Abstract: This study investigated the efficacy of a novel lidocaine-chitosan-barium titanate microemulsion gel for prolonged local anesthesia. The lidocaine microemulsion comprised 5% (w/w) lidocaine, linoleic acid (LA), chitosan, barium titanate (BaTiO3), Cremophor RH40, Tween 20, and water. Dynamic light scattering was utilized to analyze the particle size of the prepared microemulsions. The optimized microemulsion was transformed into a microemulsion gel to extend the duration of the microemulsion when administered to specific areas. Virgin oil was used as an auxiliary oil to increase the microemulsion area, allowing for a reduced amount of surfactant. *In vitro* analysis was conducted to evaluate the release of lidocaine from the microemulsion. The lidocaine/chitosan/BaTiO3 ranged in size from 7-30 nm, displaying a narrow particle size distribution. The polydispersity index (PDI) value was 0.989. Lidocaine/chitosan with BaTiO3 nanoparticles as a carrier achieved over 84% drug release, whereas the lidocaine/chitosan without the BaTiO3 nanoparticles only reached 52% cumulative release. At the concentrations used, the lidocaine-loaded chitosan and lidocaine-loaded chitosan with BaTiO3 showed a moderate effect on cellular viability. In conclusion, a new formulation of lidocaine microemulsions containing chitosan and BaTiO3 was developed and utilized to deliver lidocaine through the skin to achieve topical anesthesia.

Keywords: lidocaine, chitosan, barium titanate (BaTiO3), microemulsion, local anesthesia

INTRODUCTION

Patients often endure intense localized pain following surgical treatment. However, the duration of action for local anesthesia is typically limited to less than two hours, posing a significant challenge for effective pain management [1-4]. Therefore, it is essential to apply managed local pain therapy to effectively alleviate the economic and physical obstacles faced by patients and their caretakers [5]. The currently available dosage forms, such as gels, creams, ointments, and injections, do not fulfill the clinical requirements for achieving a desirable duration of action exceeding two hours. Patients are often hospitalized when they require infusions and multiple injections. In addition to the pain that may be felt at the injection site, there is an increased likelihood of infection and potential damage to the surrounding tissues [6,7]. To overcome these issues, medical practitioners employ various methods, including multiple injections or continuous infusions of local anesthetics. However, this approach is not without limitations. These restrictions include the discomfort experienced during injections and the elevated cost associated with continuous infusion [8-11].

Local anesthesia is important in various medical procedures, providing temporary pain relief to specific body areas. However, the need for prolonged local anesthesia has become increasingly recognized in clinical practice, particularly for complex surgeries and chronic pain management. Current formulations of local anesthetics, while effective for short-term pain control, are often limited in terms of duration and efficacy, leading to the search for innovative solutions that can offer extended pain relief with improved outcomes. One of the primary challenges with traditional local anesthetics is their relatively short duration of action, which may necessitate multiple injections or supplementary medications to maintain pain control over an extended period [9-10].

Techniques to increase the dermal flux include iontophoresis and laser/ultrasound treatment. However, these methods require specialized devices and the involvement of qualified personnel, resulting in higher expenses. Currently, local anesthetics are administered alongside adjuvants such as epinephrine, clonidine, or dexamethasone to extend their local anesthetic action [12-14]. Additionally, various vesicular drug delivery systems, such as microspheres [15, 16], microemulsions, microcrystals [17-20], micelles [21], and polymeric nanoparticles like chitosan and $BaTiO_3$ [22], are employed to optimize the delivery and effectiveness of these local anesthetics. However, the duration of activity is inconsistent when adjuvants are used, and each drug delivery system has its limitations [23].

Lidocaine, or 2-6 xylidine, is a frequently used local anesthetic clinical practice for the management of pain [24,25]. Its quick-acting nature and intermediate duration of action can be attributed to its low protein binding capacity. By binding to the voltage-gated sodium channel, lidocaine effectively inhibits the conduction of pain stimuli from sensory neurons to the central nervous system. The application of novel drug delivery systems can enhance this effect by providing a sustained release of lidocaine after topical administration [26-28]. The present study evaluated various parameters of the lidocaine microemulsion, including refractive index, cytotoxicity, droplet size, zeta potential, pH, and thermostability. We investigated the efficacy of a novel lidocaine-chitosan-barium titanate microemulsion gel for prolonged local anesthesia. Specifically, the researchers developed a new formulation of lidocaine microemulsions containing chitosan and $BaTiO_3$ and evaluated its ability to deliver lidocaine through the skin to achieve topical anesthesia.

MATERIALS AND METHODS

Ethics statement

This study was approved by the Ethical Committee of Ankang Central Hospital.

Materials

Lidocaine, chloramphenicol, poly(ε-caprolactone), linoleic acid (LA), chitosan, barium Titanate ($BaTiO_3$) nanopowder, polyoxyl 40 hydrogenated castor oil (RH40), polysorbate 20 (Tween 20), sodium hydroxide (NaOH), Carbopol 940 polymer, and phosphate-buffered saline (PBS), were purchased from Merk, Germany. MTT reagents were purchased from Sigma Aldrich, USA. All other chemicals were of analytical grade or high-performance liquid chromatography (HPLC) grade and used without further purification. Saline solution served as the control, allowing for comparison against the lidocaine-based microemulsion droplets, highlighting the unique properties of the microemulsion formulation.

Preparation of lidocaine-chitosan-nanoparticles microemulsion

The lidocaine microemulsion consists of lidocaine 5% (w/w), linoleic acid (LA), chitosan, $BaTiO_3$, Cremophor RH40, Tween 20, and water. The mixed oil phase (O) was prepared by combining LA at a 1:4 ratio. This was mixed with RH40 at 1:4, 1:1, and 4:1 ratios to obtain mixed oils. Virgin oil was used as an auxiliary oil to increase the microemulsion area, allowing for a reduced amount of surfactant. The mixed surfactant (S) was prepared by mixing RH40 and Span 80 at a 5:1 (w/w) ratio. This improved the solubility of the surfactant, increased the microemulsion area, and reduced the amount of surfactant. Microemulsions containing lidocaine were prepared by dissolving 5% lidocaine (w/w), chitosan, and BaTiO3 in various mixtures at room temperature, followed by slow addition with magnetic stirring.

To initiate the preparation process, the primary components of the microemulsion gel were carefully chosen to create a well-balanced formulation with optimal characteristics for sustained drug release and enhanced bioavailability. These components typically included: oils with good spreading properties and high drug solubility, such as medium-chain triglycerides or lipid-based carriers, chosen to ensure effective drug loading and release. Surfactants are essential for stabilizing the emulsion and promoting the formation of small droplets to enhance drug dispersion. Non-ionic surfactants, such as RH40 and Span 80, were employed due to their compatibility with various drugs and ability to reduce interfacial tension.

Preparation of the lidocaine-chitosan-nanoparticle microemulsion

A dynamic light scattering apparatus (Zetasizer Nano S90, Malvern Instruments, UK) was utilized to analyze the particle size of the prepared microemulsions. The measurements were made at room temperature. A transmission electron microscope (JEM1200EX, JEOL, Tokyo, Japan) was used to observe the surface morphology of the lidocaine/chitosan/$BaTiO_3$ microemulsions. A copper grid was loaded with a drop of microemulsions and subsequently stained with a phosphotungstic acid solution (2%, w/v). Following air-drying at room temperature, the samples were examined by transmission electron microscopy. The diluted ointment was applied onto a copper grid coating by soaking for 1 min. The specimens were stained with a 1% (w/v) phosphotungstic acid for 10 s. The sample was air-dried at 25°C for 3 h. Images were captured using a LIBRA 120 device (Carl Zeiss in Oberkochen, Germany), with an acceleration voltage of 200 kV.

pH measurement

One gram of lidocaine-chitosan-$BaTiO_3$ was mixed with 99 g of distilled water and stirred thoroughly until a uniform mixture was obtained. The pH was measured in triplicate, using a calibrated pH meter.

Preparation of the microemulsion gel

The optimized microemulsion was transformed into a microemulsion gel to extend the duration of microemulsions when administered to specific areas. This was achieved by dispersing 0.5% w/w of Carbopol® 940 into the prepared microemulsion system while subjecting it to magnetic stirring. Subsequently, the gel was neutralized until a thick and transparent hydrogel was formed.

Tensile strength and elongation at break

The TA-XT Plus Texture Analyzer (Stable Micro Systems, Surrey, England) was utilized to determine the tensile strength (TS) and elongation at break (EB). Strips of the lidocaine microemulsion gels, measuring 1 cm in width and 5 cm in length were affixed to the lower and upper ends of the analytical probe. The distance between the strips was 3.5 cm. The elongation rate was 10 mm/s, and the load cell capacity was 50 kg. Measurements were conducted in triplicate at a temperature of 25°C.

In vitro drug release of lidocaine

The release behavior of lidocaine was investigated by *in vitro* drug release studies using the dialysis method. Lidocaine (1 mL) was enclosed in a semipermeable dialysis membrane with a molecular weight cutoff of 50 kDa. Lidocaine has a molecular weight of 234.34 g/mol or 0.23 kDa. This is significantly lower than 50 kDa of the dialysis membrane used. Accordingly, a 50 kDa membrane would effectively retain these larger molecular weight excipients inside the dialysis bag, allowing the relatively small lidocaine molecule to permeate through the membrane into the release medium. These dialysis bags were then submerged in PBS (pH 7.4) and kept at 37°C with continuous stirring. At specific time intervals (0, 6, 10, 16, 20, 24, 26, and 30 h), a predetermined volume of samples (0.5 mL) was collected from the dissolution media, and an equal volume of fresh buffer solution (0.5 mL) was added. The collected samples were subsequently analyzed to determine the amount of lidocaine released.

In vitro cytotoxicity of lidocaine-based microemulsion gel

The cytotoxicity of lidocaine/chitosan/ $BaTiO_3$ microemulsion gel was assessed *in vitro* using fetal rat skin keratinocytes (FRSK) by the MTT assay. A microemulsion gel containing lidocaine/chitosan/$BaTiO_3$ and free lidocaine was prepared at a concentration of 10 mg/mL. FRSK cells (1×10^6) were cultured in 96-well plates and incubated for 1, 7, and 14 days. Subsequently, different concentrations of the samples were added to each well. The cells were analyzed by incubating with MTT solution (25 µL, 5 mg/mL) for 2 h at 37°C. The amount of formazan produced from the conversion of MTT was measured using a microplate reader (Bio-Rad, Hercules, CA, USA) at a wavelength of 630 nm to determine the percentage of viable cells.

Thermodynamic stability studies

Lidocaine microemulsions were evaluated for thermodynamic stability. To ensure miscibility, clarity, and no drug precipitation, microemulsions were subjected to (i) centrifugation tests (3500 rpm for 30 min), (ii) heating/cooling cycles (six cycles at 45°/4°C for 2 days), and (iii) freeze/thaw (three cycles at 25°/-20°C cycles for 2 days).

Statistical analysis

Statistical analysis was conducted using GraphPad Prism 8.0 and SPSS v.24. The mean±standard deviation (SD) was used to express all values. Two-tailed t-tests were employed to compare two groups, while one-way ANOVA was utilized for several groups after conducting the normality test. A P value <0.05 was considered significant.

RESULTS

Preparation and characterization of the lidocaine/chitosan/$BaTiO_3$ microemulsion

The mean microemulsion droplet size and zeta potential measurements are shown in Supplementary Table S1. The lidocaine/chitosan/$BaTiO_3$ microemulsion was in the range of 7-30 nm with a narrow particle size distribution pattern (Fig. 1). The average droplet sizes of the lidocaine/chitosan/$BaTiO_3$ microemulsion were 15 nm. The polydispersity index (PDI) value was 0.989, indicating a narrow size distribution for microemulsion formulation. These findings illustrate the small particle size and uniformity of the microemulsion droplets, rendering them suitable for dermal/transdermal delivery. The TEM analysis revealed the morphologies of the microemulsion droplets containing lidocaine/chitosan/$BaTiO_3$ in the formulation. Supplementary Fig. S1 illustrates that the TEM images displayed uniform spherical globules of the microemulsion, indicating the absence of any aggregation.

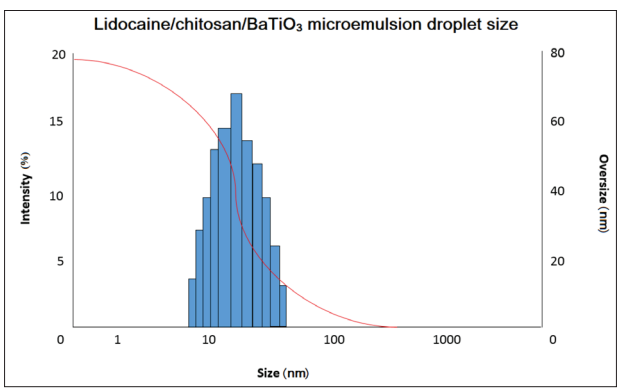

Fig.1. Particle size distribution of the lidocaine/chitosan/$BaTiO_3$ microemulsion. Using DLS, the microemulsion exhibits a size range of 7-30 nm, with an average droplet size of 15 nm. It has a narrow size distribution and uniformity of the microemulsion droplets, as indicated by a PDI value of 0.989. Oversize demonstrates the presence of larger droplets or particles than what is intended in a microemulsion.

Drug-release of the lidocaine-chitosan-BaTiO3 microemulsion gel

Fig. 2 demonstrates that within 30 h, the lidocaine/chitosan with the $BaTiO_3$ nanoparticles as a carrier, achieved over 84% drug release, whereas lidocaine/chitosan without $BaTiO_3$ nanoparticles only reached 52% cumulative release. This observation provides evidence for the presence of the $BaTiO_3$ molecule in lidocaine microemulsions, which contributes to a more sustained release in the system.

Cytotoxicity of lidocaine-loaded microemulsion gels

In vitro cytotoxicity of lidocaine/chitosan/$BaTiO_3$ was tested by evaluating FRSK cell viability (Fig. 3). At the concentrations used, the lidocaine-loaded chitosan and lidocaine-loaded chitosan with $BaTiO_3$ showed a moderate effect on cellular viability, with values slowly decreasing from 90% to 80%. The microemulsion gels composed of lidocaine/chitosan with or without $BaTiO_3$ provided an ideal and non-toxic environment.

Mechanical properties of the lidocaine-loaded nanoparticle

To investigate the mechanical properties, two parameters, tensile strength (TS) and during fiber breakage, were considered. As shown in Supplementary Table S2, the TS of 2% lidocaine-chitosan-$BaTiO_3$, 5% lidocaine-chitosan-$BaTiO_3$, and lidocaine were 0.3±0.05, 0.26±0.06, and 0.2±0.07 MPa, respectively. The elongation at break (EB) of 2% lidocaine-chitosan-$BaTiO_3$, 5% lidocaine-chitosan-$BaTiO_3$, and lidocaine were 25±3, 21±4, and 8±2.5, respectively. By adding BaTiO,

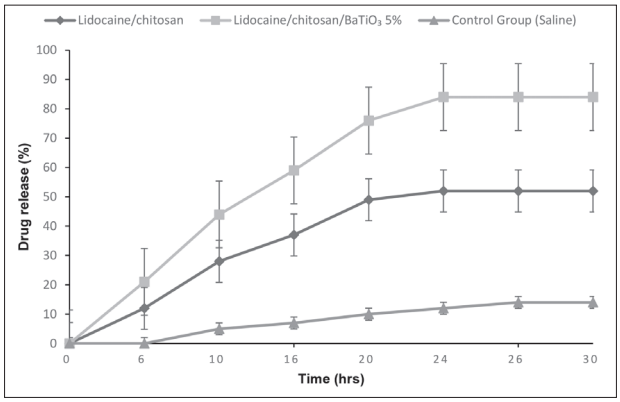

Fig.2. Cumulative lidocaine drug release profiles at various time intervals (0, 6, 10, 16, 20, 24, 26, and 30 h). *In vitro* drug release was studied using the dialysis method. Within 24 h, the lidocaine/chitosan/$BaTiO_3$ formulation achieved over 84% cumulative drug release and remained constant until 30 h. In contrast, the formulation without $BaTiO_3$ only reached 52% release.

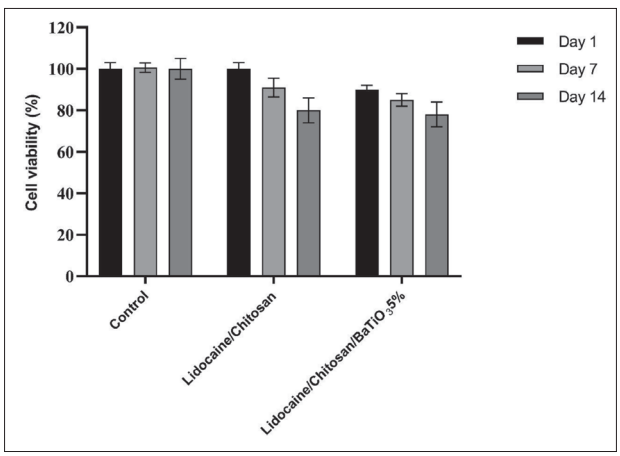

Fig.3. Cytotoxicity assessment of lidocaine/chitosan/$BaTiO_3$ microemulsion gel on FRSK cells. MTT assay assessed the cytotoxicity of lidocaine/chitosan and lidocaine/chitosan/$BaTiO_3$ on FRSK cells. Cell viability was above 80% at of 10 mg/mL for both formulations. No significant decrease in cell proliferation was observed compared to the control groups, indicating the safety of the formulations. Data is presented as the mean±SD. $P<0.05$ was considered as statistically significant.

the ultimate tensile strength (UTS), and EB decreased. These changes were not significant, which means that the $BaTiO_3$ nanoparticles do not significantly affect the UTS and EB properties ($P>0.05$) (Supplementary Table S2).

Thermodynamic stability results

The optimized lidocaine/chitosan/$BaTiO_3$ microemulsions were physically stable after successfully passing the thermodynamic stability studies (Supplementary Table S2).

DISCUSSION

Nanomaterials have gained attention due to their excellent biocompatibility and controllability, and have shown significant potential in serving as advanced drug carriers [29]. The objective of this study was to investigate the efficacy of a novel lidocaine-chitosan-barium titanate microemulsion gel in achieving prolonged local anesthesia. The size of the droplets in the microemulsion gels plays a crucial role in determining their properties. Smaller droplet sizes, ranging from 5 to 500 nm, have been found to effectively penetrate the stratum corneum barrier and facilitate drug delivery [30]. In our study, the lidocaine/chitosan/BaTiO3 exhibited nanometer-sized particles ranging from 7 to 30 nm and showed a narrow particle size distribution pattern.

The utilization of nanoparticles as drug-eluting devices is a relatively new approach. Drugs can be dispersed directly in the membrane matrix or encapsulated within nanoparticles, which are then incorporated into the matrix. The latter approach offers advantages such as reducing drug toxicity and prolonging drug release. Drug-loaded nanoparticles can interact with biomembranes and local tissues through physicochemical binding [31]. Studies have shown that nanocarrier properties can explain the enhanced permeation ability of lidocaine/chitosan/$BaTiO_3$ for delivery. The microemulsion gels with small sizes ensure close contact, thereby leading to an increased quantity of encapsulated drugs in the tissue [32]. The lidocaine/chitosan with $BaTiO_3$ nanoparticles as a carrier has achieved over 84% drug release, whereas lidocaine/chitosan without the $BaTiO_3$ nanoparticles only reached 52% cumulative release. Additionally, at the concentrations used, lidocaine-loaded chitosan and lidocaine-loaded chitosan with $BaTiO_3$ showed a moderate effect on cellular viability. Lidocaine concentrations of 0.75% and higher cause significant decreases in cell viability compared with the control saline solution and their cytotoxicity was comparable to the standard agent melphalan (0.5%) after 24 and 72 h [33]. The type of cell death induced by local anesthetics appears to be influenced by the duration of exposure, concentration,

and the specific type of anesthetic used. Research suggests that bupivacaine primarily leads to necrosis, while lidocaine predominantly triggers apoptosis [34,35].

The mechanical properties of the lidocaine-loaded nanostructured microemulsion gels, specifically the tensile strength (TS) and elongation at break (EB) were analyzed. The TS and EB decreased slightly after adding $BaTiO_3$ nanoparticles to the lidocaine-chitosan formulation; however, these changes were not statistically significant ($P>0.05$), indicating that the addition of $BaTiO_3$ nanoparticles did not significantly affect the mechanical properties of the microemulsion gel. The addition of nanoparticles to the microemulsion gel changes the physical, chemical, and mechanical characteristics and structure. In this study, the introduction of $BaTiO_3$ and chitosan did not impact the physical and mechanical properties of the microemulsion containing lidocaine. However, it did affect the morphology of the system. The positively charged amines in the chitosan chains strongly interacted with the negatively charged functional groups in the lidocaine chains, forming a polyelectrolyte complex (PEC). The PEC acted as a gel for the microemulsion, providing a suitable environment for the incorporation of drug-loaded nanoparticles [36,37]. The physical and mechanical findings affect the optimization of the nanoparticle formulation for drug delivery purposes. For example, a narrow particle size distribution and optimal size range can enhance the nanoparticles' ability to reach target sites within the body, improve cellular uptake, and facilitate controlled drug release. Similarly, a favorable zeta potential can contribute to the stability of the formulation, prevent particle aggregation, and maintain the desired characteristics of the nanoparticles during storage and administration [28,29].

$BaTiO_3$ nanoparticles can act as solubilizing agents within the microemulsion, increasing the solubility and loading capacity of the drug (e.g. lidocaine) in the formulation. The nanoparticles' high surface area and adsorption capacity help solubilize the drug in the microemulsion. The $BaTiO_3$ nanoparticles can interact with the drug molecules and the microemulsion components to modulate the drug release kinetics. The nanoparticles may slow down the diffusion of the drug out of the microemulsion, leading to more controlled and sustained release [27,33].

A primary safety concern associated with barium titanate is its potential for skin irritation or sensitization after dermal exposure. It is crucial to investigate the likelihood of adverse skin reactions, such as irritation or allergic responses, that may result from the presence of barium titanate in the topical formulation. Additionally, the potential for skin penetration and systemic absorption of barium titanate particles should be carefully assessed to determine the risk of systemic exposure and any associated toxic effects [34].

CONCLUSIONS

In this study, a novel formulation of lidocaine microemulsions enriched with chitosan and $BiTo_3$ was developed and applied to facilitate the transdermal delivery of lidocaine for achieving effective topical anesthesia. The *in vitro* evaluation of skin permeation demonstrated that the utilization of microemulsions significantly enhances the transdermal penetration of lidocaine, underscoring the potential of microemulsions as an efficient drug delivery system for dermatological applications. Moreover, the results obtained from mechanical analysis and fluorescence microscopy provided compelling evidence supporting the efficacy of microemulsions as a promising approach to surmount the skin's natural protective barrier. The ability of microemulsions to effectively deliver lidocaine through the skin, as revealed by this study, suggests their valuable role in enhancing the permeation of therapeutic agents across the skin barrier for improved therapeutic outcomes. Overall, the incorporation of lidocaine-based mixtures into microemulsions represents an appealing and promising strategy for future developments in topical anesthetic therapy. The successful utilization of microemulsions highlights their potential as a delivery vehicle for enhancing drug permeation, underscoring their versatility and efficacy in overcoming skin barriers for targeted and efficient delivery of therapeutic agents. Further research and clinical investigations are warranted to explore the full potential and optimize the formulation parameters of lidocaine microemulsions for topical anesthesia, to advance the development of innovative and effective strategies for pain management and localized anesthesia.

Funding: No specific funding was received for this work.

Author contributions: Conceptualization, LL, and XQ; methodology, LL; software, XQ; validation, LL; formal analysis, XQ; investigation, LL; visualization, XQ; supervision, LL; project administration, LL. Both authors have read and agreed to the published version of the manuscript.

Conflict of interest disclosure: The authors declare no potential conflicts of interest.

Data availability: Data underlying the reported findings have been provided as a raw dataset available here: https://www.serbiosoc.org.rs/NewUploads/Uploads/Qiao%20and%20Li_Raw%20Dataset.pdf

REFERENCES

1. Carvalho G, Nikkhah G, Samii M. Pain management after post-traumatic brachial plexus lesions. Conservative and surgical therapy possibilities. Der Orthopade. 1997;26(7):621-5. https://doi.org/10.1007/s001320050132
2. Gordon SM, Mischenko AV, Dionne RA. Long-acting local anesthetics and perioperative pain management. Dent Clin North Am. 2010;54(4):611-20. https://doi.org/10.1016/j.cden.2010.06.002
3. Markman JD, Philip A. Interventional approaches to pain management. Anesthesiol Clin. 2007;25(4):883-98. https://doi.org/10.1016/j.anclin.2007.07.012
4. Golzari SE, Soleimanpour H, Mahmoodpoor A, Safari S, Ala A. Lidocaine and pain management in the emergency department: a review article. Anesth Pain Med. 2014;4(1):e15444. https://doi.org/10.5812/aapm.15444
5. Epstein-Barash H, Shichor I, Kwon AH, Hall S, Lawlor MW, Langer R, Kohane, D. Prolonged duration local anesthesia with minimal toxicity. Proc Natl Acad Sci U S A. 2009;106(17):7125-30. https://doi.org/10.1073/pnas.0900598106
6. Lehr VT, Taddio A. Topical anesthesia in neonates: clinical practices and practical considerations. Semin Perinatol. 2007;31(5):323-9. https://doi.org/10.1053/j.semperi.2007.07.008
7. Ogle OE, Mahjoubi G. Local anesthesia: agents, techniques, and complications. Dent Clin North Am. 2012;56(1):133-48. https://doi.org/10.1016/j.cden.2011.08.003
8. Zink W, Bohl JR, Hacke N, Sinner B, Martin E, Graf BM. The long term myotoxic effects of bupivacaine and ropivacaine after continuous peripheral nerve blocks. Anesth Analg. 2005;101(2):548-54. https://doi.org/10.1213/01.ANE.0000155956.59842.0A
9. Barletta JF. Clinical and economic burden of opioid use for postsurgical pain: focus on ventilatory impairment and ileus. Pharmacotherapy. 2012;32(9pt2):12S-18S. https://doi.org/10.1002/j.1875-9114.2012.01178.x
10. Ilfeld BM. Continuous peripheral nerve blocks: a review of the published evidence. Anesth Analg. 2011;113(4):904-25. https://doi.org/10.1213/ANE.0b013e3182285e01
11. Kerr DR, Kohan L. Local infiltration analgesia: a technique for the control of acute postoperative pain following knee and hip surgery: a case study of 325 patients. Acta Orthop. 2008;79(2):174-83. https://doi.org/10.1080/17453670710014950
12. Quandt JE. Anesthetic considerations for laser, laparoscopy, and thoracoscopy procedures. Clin Tech Small Anim Pract. 1999;14(1):50-5. https://doi.org/10.1016/S1096-2867(99)80027-9
13. Culp Jr WC, Culp WC. Practical application of local anesthetics. J Vasc Interv Radiol. 2011;22(2):111-8. https://doi.org/10.1016/j.jvir.2010.10.005
14. Movafegh A, Razazian M, Hajimaohamadi F, Meysamie A. Dexamethasone added to lidocaine prolongs axillary brachial plexus blockade. Anesth Analg. 2006;102(1):263-7. https://doi.org/10.1213/01.ane.0000189055.06729.0a
15. Alshehri S, Karan R, Ghalayini S, Kahin K, Khan Z, Renn D, Mathew S, Rueping M, Hauser, C. Air-loaded gas vesicle nanoparticles promote cell growth in three-dimensional bioprinted tissue constructs. Int J Bioprint. 2022;8(3):489. https://doi.org/10.18063/ijb.v8i3.489
16. Sarvari P, Sarvari P. Advances in nanoparticle-based drug delivery in cancer treatment. Glob Transl Med. 2023;2:0394. https://doi.org/https://doi.org/10.36922/gtm.0394
17. Boedeker BH, Lojeski EW, Kline MD, Haynes DH. Ultra-Long-Duration Local Anesthesia Produced by Injection of Lecithin-Coated Tetracaine Microcrystals. J Clin Pharmacol. 1994;34(6):699-702. https://doi.org/10.1002/j.1552-4604.1994.tb02026.x
18. Majd MH. Dual-targeting and specific delivery of tamoxifen to cancer cells by modified magnetic nanoparticles using hyaluronic acid and folic acid. Tumor Discov. 2022;1(1):41. https://doi.org/https://doi.org/10.36922/td.v1i1.41
19. Yusoff MS, Gopinath SC, Uda M, Lakshmipriya T, Yaakub ARW, Anbu P. Conjugation of silver and gold nanoparticles for enhancing antimicrobial activity. INNOSC Theranostics Pharmacol Sci. 2022;4:38-47.
20. Martínez-Pérez D, Guarch-Pérez C, Purbayanto MAK, Choińska E, Riool M, Zaat SA, Wojciech Ś. 3D-printed dual drug delivery nanoparticle-loaded hydrogels to combat antibiotic-resistant bacteria. Int J Bioprint. 2023;9(3):683. https://doi.org/10.18063/ijb.683
21. Maulvi FA, Parmar RJ, Desai AR, Desai DM, Shukla MR, Ranch KM, Shah SA, Shah DO. Tailored gatifloxacin Pluronic® F-68-loaded contact lens: addressing the issue of transmittance and swelling. Int J Pharm. 2020;581:119279. https://doi.org/10.1016/j.ijpharm.2020.119279
22. Beiranvand S, Eatemadi A, Karimi A. New updates pertaining to drug delivery of local anesthetics in particular bupivacaine using lipid nanoparticles. Nanoscale Res Lett. 2016;11:1-10. https://doi.org/10.1186/s11671-016-1520-8
23. de Paula E, Cereda CM, Fraceto LF, de Araujo DR, Franz-Montan M, Tofoli GR, Ranali J, Volpato MC, Groppo FC. Micro and nanosystems for delivering local anesthetics. Expert Opin Drug Deliv. 2012;9(12):1505-24. https://doi.org/10.1517/17425247.2012.738664
24. Moller R, Covino BG. Cardiac electrophysiologic properties of bupivacaine and lidocaine compared with those of ropivacaine, a new amide local anesthetic. Anesthesiology. 1990;72(2):322-9. https://doi.org/10.1097/00000542-199002000-00019

25. Abou-Okeil A, Rehan M, El-Sawy S, El-Bisi M, Ahmed-Farid O, Abdel-Mohdy F. Lidocaine/β-cyclodextrin inclusion complex as drug delivery system. Euro Poly J. 2018;108:304-10.
26. Pipa-Vallejo A, García-Pola-Vallejo MJ. Local anesthetics in dentistry. Med Oral Patol Oral Cir Bucal. 2004;9(5):438-43.
27. You P, Yuan R, Chen C. Design and evaluation of lidocaine-and prilocaine-coloaded nanoparticulate drug delivery systems for topical anesthetic analgesic therapy: a comparison between solid lipid nanoparticles and nanostructured lipid carriers. Drug Des Devel Ther. 2017:2743-52. https://doi.org/10.2147/DDDT.S141031
28. de Paula E, Cereda C, Tofoli GR, Franz-Montan M, Fraceto LF, De Araújo DR. Drug delivery systems for local anesthetics. Recent Pat Drug Deliv Formul. 2010;4(1):23-34. https://doi.org/10.2174/187221110789957228
29. Morihama ACD, Mierzwa JC. Clay nanoparticles effects on performance and morphology of poly (vinylidene fluoride) membranes. Braz J Chem Eng. 2014;31:79-93. https://doi.org/10.1186/x12781-016-1520-8
30. Tartaro G, Mateos H, Schirone D, Angelico R, Palazzo G. Microemulsion microstructure (s): A tutorial review. Nanomaterials. 2020;10(9):1657. https://doi.org/10.3390/nano10091657
31. Xu C, Cao Y, Lei C, Li Z, Kumeria T, Meka AK, Xu J, Liu J, Yan C, Luo L. Polymer–mesoporous silica nanoparticle core–shell nanofibers as a dual-drug-delivery system for guided tissue regeneration. ACS App Nano Mater. 2020;3(2):1457-67. https://doi.org/10.1021/acsanm.9b02298
32. Jaramillo N, Paucar C, Fernández A, Negrete CG, García C. Microemulsion assisted sol-gel method as approach to load a model anticancer drug inside silica nanoparticles for controlled release applications. Coll Interface Sci Commu. 2018;24:13-7. https://doi.org/10.2147/x123.S141031
33. Kang D-K, Zhao L-Y, Wang H-L. Cytotoxic effects of local anesthesia through lidocaine/ropivacaine on human melanoma cell lines. Rev Bras Anestesiol. 2016;66:594-602. https://doi.org/10.1016/j.bjan.2016.08.002
34. Breu A, Scheidhammer I, Kujat R, Graf B, Angele P. Local anesthetic cytotoxicity on human mesenchymal stem cells during chondrogenic differentiation. Knee Surg Sports Traumatol Arthrosc. 2015;23:937-45. https://doi.org/10.1007/s00167-014-3312-y
35. Wu T, Smith J, Nie H, Wang Z, Erwin PJ, Van Wijnen AJ, Qu W. Cytotoxicity of local anesthetics in mesenchymal stem cells. Am J Phys Med Rehabil. 2018;97(1):50-5. https://doi.org/10.1097/PHM.0000000000000837
36. Hasan S, Thomas N, Thierry B, Prestidge CA. Controlled and localized nitric oxide precursor delivery from chitosan gels to Staphylococcus aureus biofilms. J Pharm Sci. 2017;106(12):3556-63. https://doi.org/10.1016/j.xphs.2017.08.006
37. Nath SD, Abueva C, Kim B, Lee BT. Chitosan–hyaluronic acid polyelectrolyte complex scaffold crosslinked with genipin for immobilization and controlled release of BMP-2. Carbohydr Polym. 2015;115:160-9. https://doi.org/10.1016/j.carbpol.2014.08.077
38. Xiang Z, Xu L, Shan Y, Cui X, Shi B, Xi Y, Ren P, Zheng X, Zhao C, Luo D, Li Z. Tumor microenviroment-responsive self-assembly of barium titanate nanoparticles with enhanced piezoelectric catalysis capabilities for efficient tumor therapy. Bio Mater. 2024;1;33:251-61. https://doi.org/10.1016/j.bioactmat.2023.11.004
39. Onorato GD, Amaral DL, Oliveira LF, Brandao HD, Munk M. Barium Titanate Nanoparticles Exhibit Cytocompatibility in Cultured Bovine Fibroblasts: A Model for Dermal Exposure. Cur J App Sci Tech. 2024;43(5):1-10. https://doi.org/10.9734/cjast/2024/v43i54372

SUPPLEMENTARY MATERIAL

Supplementary Table S1. Comparison of particle size, poly-dispersibility index, and zeta potential of lidocaine/chitosan/barium titanate ($BaTiO_3$) at 2% and 5% concentrations, and saline control group; data are presented as the mean±standard deviation). The table provides a detailed comparison of the key physicochemical properties of the formulations studied, including particle size, poly-dispersibility index (PDI), and zeta potential.

Lidocaine Microemulsions	Particle size (nm)	Poly-dispersibility index	Zeta potential (mV)
Control Group (Saline)	103.13	0.14	+8.67
Lidocaine/Chitosan/ $BaTiO_3$ 2%	16±2.2	0.966	-24.5±4.6
Lidocaine/Chitosan/ $BaTiO_3$ 5%	13±1.1	0.989	-27.2±5.1

Supplementary Table S2. Mechanical properties of lidocaine-loaded microemulsion.

Samples	UTS (MPa)	Elongation at break (%)
lidocaine-chitosan- $BaTiO_3$ 2%	0.3±0.05	25±3
lidocaine-chitosan- $BaTiO_3$ 5%	0.26±0.06	21±4
Lidocaine	0.2±0.07	8±2.5

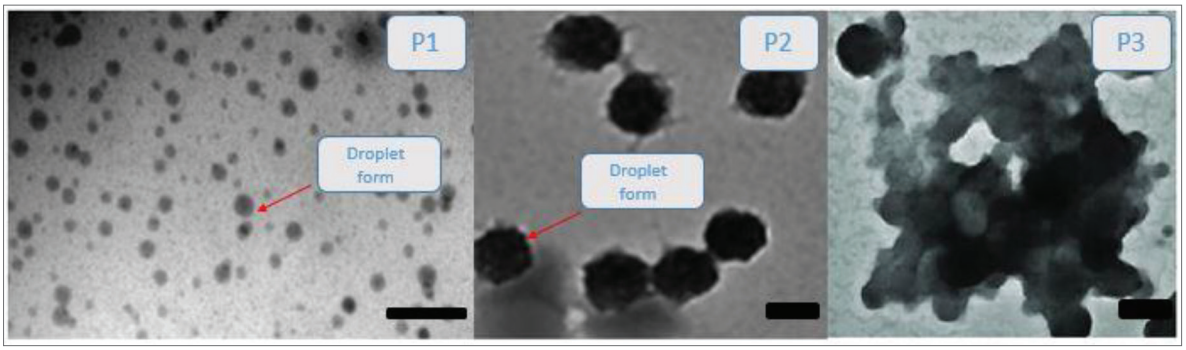

Supplementary Fig. S1. Transmission electron microscopy (TEM). TEM images reveal nanoparticles in the lidocaine microemulsion. The TEM image is magnified ×20,000, with each scale bar representing 400 nm. P3 does not form a droplet and exhibits non-uniform size distribution, whereas P2 and P3 display a uniform droplet morphology in the microemulsion.